

Why Not Use Your Textbook? Knowledge-Enhanced Procedure Planning of Instructional Videos

Kumaranage Ravindu Yasas Nagasinghe¹, Honglu Zhou², Malitha Gunawardhana^{1,3},
 Martin Renqiang Min², Daniel Harari⁴, Muhammad Haris Khan¹
¹MBZUAI, ²NEC Laboratories, USA, ³ University of Auckland, ⁴Weizmann Institute of Science

Abstract

In this paper, we explore the capability of an agent to construct a logical sequence of action steps, thereby assembling a strategic procedural plan. This plan is crucial for navigating from an initial visual observation to a target visual outcome, as depicted in real-life instructional videos. Existing works have attained partial success by extensively leveraging various sources of information available in the datasets, such as heavy intermediate visual observations, procedural names, or natural language step-by-step instructions, for features or supervision signals. However, the task remains formidable due to the implicit causal constraints in the sequencing of steps and the variability inherent in multiple feasible plans. To tackle these intricacies that previous efforts have overlooked, we propose to enhance the agent’s capabilities by infusing it with procedural knowledge. This knowledge, sourced from training procedure plans and structured as a directed weighted graph, equips the agent to better navigate the complexities of step sequencing and its potential variations. We coin our approach KEPP, a novel Knowledge-Enhanced Procedure Planning system, which harnesses a probabilistic procedural knowledge graph extracted from training data, effectively acting as a comprehensive textbook for the training domain. Experimental evaluations across three widely-used datasets under settings of varying complexity reveal that KEPP attains superior, state-of-the-art results while requiring only minimal supervision. Code and trained model are available at <https://github.com/Ravindu-Yasas-Nagasinghe/KEPP>

1. Introduction

The evolution of the internet has precipitated an unprecedented influx of video content, serving as a vital educational resource for myriad learners. Individuals frequently leverage platforms such as YouTube to acquire new skills, ranging from culinary arts to automobile maintenance [33].

¹Mohamed bin Zayed University of Artificial Intelligence

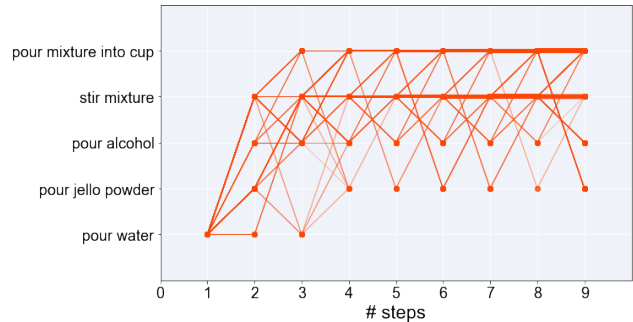


Figure 1. **Expert trajectories [7] of the ‘Make Jello Shots’ task from the CrossTask dataset [59].** Heavier color indicates more frequently visited path. This depicts the complexities of the procedure planning task, arising from the subtle causal links in step sequencing (e.g., steps like ‘stir mixture’ or ‘pour mixture’ typically occur after adding individual ingredients), the varied probabilities of transitioning between steps, and the diversity in plans viable for a given starting point and an intended outcome. Motivated by these nuanced challenges, we propose Knowledge-Enhanced Procedure Planning (KEPP) with the use of a probabilistic procedure knowledge graph to capture and represent these intricacies

While these instructional videos benefit the development of intelligent agents in mastering long-horizon tasks, the challenge for embodied agents like robots extends beyond merely interpreting visuals. It requires high-level reasoning and planning to effectively assist in complex, real-life scenarios [13].

Procedure Planning in Instructional Videos demands an agent to produce a sequence of actionable steps, thereby crafting a procedure plan that facilitates the transition from an initial visual observation towards achieving a desired goal state [7, 9, 46, 49, 50, 55]. The task acts as a precursor to an envisioned future scenario in which an agent like a robot provides on-the-spot support, such as assisting an individual in preparing a recipe. The capacity to perceive the state of the world and devise coherent action plans in conjunction with or on behalf of humans appears indispensable in such contexts [6].

Current methods in procedure planning in instructional videos make extensive use of various annotations available within the datasets to enrich input features or provide supervisory signals (see Table 1). These include detailed, temporally localized visual observations of intermediate action steps throughout the procedure plan [7, 9, 46], high-level procedural task labels [49, 50], and step-by-step instructions in natural language [49, 55]. Despite advancements, significant challenges persist, including characterizing the implicit causal constraints in step sequencing, the varied probabilities of transitioning between steps, and the inherent variability of multiple viable plans (see Fig. 1).

To address these intricacies that previous efforts have overlooked, we propose to enhance the agent’s capabilities in procedure planning by infusing it with comprehensive procedural knowledge [58], derived from training procedure plans and structured as a directed weighted graph. This graph, as a Probabilistic Procedural Knowledge Graph [5] where nodes denote steps from diverse tasks and edges represent step transition probabilities in the training domain, empowers agents to more adeptly navigate the complexities of step sequencing and its potential variations. We coin our proposed approach KEPP, a novel Knowledge-Enhanced Procedure Planning system that harnesses a probabilistic procedural knowledge graph (P²KG), constructed from training procedure plans. This graph functions like a detailed textbook, providing extensive knowledge for the training domain, and thereby circumventing the need for costly multiple annotations required by existing methods. Additionally, we decompose the instructional video procedure planning problem into two parts: one driven by objectives specific to step perception and the other by a procedural knowledge-informed modeling of procedure planning. In this problem decomposition, the first and last action steps are predicted based on the initial and goal visual states. Following this, a procedure plan is crafted by leveraging the procedure plan recommendations retrieved from the P²KG. The recommendations correspond to the most probable procedure plans frequently used in training, conditioned on the predicted first and last action steps. In a similar vein to the approach by Li *et al.* [29], our proposed decomposition strategy reduces uncertainty by maximizing the use of currently available information, namely the initial and goal visual states. This allows for the improvement of procedure planning through more accurate predictions of start and end actions. Plus, this decomposition effectively incorporates procedural knowledge into procedure planning, thereby enhancing its effectiveness.

Our contributions are as follows:

- We propose KEPP, a Knowledge-Enhanced Procedure Planning system for instructional videos that leverages rich procedural knowledge from a probabilistic procedural knowledge graph (P²KG). This approach necessitates

only a minimal amount of annotations for supervision.

- We decompose the problem in procedure planning of instructional videos: predicting the initial and final steps from the start and end visuals, and then creating a plan using procedural knowledge retrieved based on these predicted steps. This approach prioritizes the currently available information and effectively incorporates procedural knowledge, enhancing strategic planning.
- Experimental evaluations conducted on three widely-used datasets, under settings of varying complexity, reveal that KEPP attains superior, state-of-the-art results in procedure planning. Code and trained models will be made publicly available.

2. Related Work

Instructional Videos, which demonstrate multi-step procedures, have become a hotbed of research. The studies delve into various aspects, including comprehending and extracting intricate spatiotemporal content from video [12, 18, 19, 21, 23, 35, 39, 40, 44, 51, 53], interpreting the interrelationships between various actions and procedural events [43, 59], and developing capabilities for forecasting [37, 38] and strategic reasoning and planning [28] within the context of these videos. Furthermore, by leveraging the multimodality of visual, auditory, and narrative elements within these videos, research extends to areas like multimodal alignment [2, 54], grounding [10, 14, 25, 32, 47], representation learning [11, 34, 57], pre-training [15, 26, 58], and more [17, 24, 36, 52]. This paper focuses on procedure planning in instructional videos.

Procedure Planning is a vital skill for autonomous agents tasked with handling complex activities in everyday settings. Essentially, these agents must discern the appropriate actions to reach a specific goal. This aspect of artificial intelligence (AI) has been a prominent and integral subject in fields like robotics [20, 28, 41, 42]. Yet, the challenge of procedure planning in the context of instructional videos is notably distinct, and potentially more complex, than its counterparts in natural language processing [8, 30], multimodal generative AI [13, 31], and simulated environments [27, 28, 41]. Its significance is underscored by the need for planning that is grounded in real-world scenes. This requires the development of AI agents capable of accurately perceiving and understanding the current real-world context, and then anticipating and mapping out a logical sequence of actions to fulfill a high-level goal effectively.

Procedure Planning in Instructional Videos has recently garnered research attention. DDN [9] initiates this trend by conceptualizing the problem as sequential latent space planning. Building on this, PlaTe [46] employs transformers for both action and state models, integrating Beam Search for enhanced performance. Meanwhile, Ext-GAIL [7] suggests employing contextual modeling through Variational

autoencoder and adversarial policy learning. This method considers contextual information as time-invariant knowledge, crucial for distinguishing specific tasks and allowing for multiple planning outcomes.

While these earlier approaches have viewed procedure planning as an autoregressive sequence generation problem, recent methods regard it as a distribution-fitting problem to mitigate error propagation in sequential decisions. In this vein, P³IV [55] replaces intermediate visual states with linguistic representations for supervision, predicting all steps simultaneously instead of using autoregressive methods. To circumvent the complex learning strategies and high annotation costs of previous work, PDPP [50] models the entire intermediate action sequence distribution using a conditioned projected diffusion model. This approach redefines the planning problem as a sampling process from this distribution and simplifies supervision by using only instructional video task labels. E3P [49], also encoding task information, adopts a mask-and-predict strategy for mining step relationships in procedural tasks, integrating probabilistic masking for regularization. Differing from these methods, our approach does not rely on annotations of intermediate states, natural language step representations, or procedural task labels.

Recognizing the difficulties inherent in high dimensional state supervision and the accumulation of errors in action sequences, SkipPlan [29] was developed. It strategically focuses on action predictions, breaking down longer sequences into shorter, more manageable sub-chains by skipping over less reliable intermediate actions. Drawing inspiration from SkipPlan, our approach decomposes the procedure planning problem to prioritize the most reliable information available (ref. § 3.1.2). However, we innovate further by incorporating a Probabilistic Procedure Knowledge Graph, significantly enriching the planning phase.

3. Methodology

In the following, we will first introduce the problem setup in § 3.1, and then, we present the details of KEPP, our novel Knowledge-Enhanced Procedure Planning system, in § 3.2. An overview of KEPP is provided in Fig. 2.

3.1. Problem and Method Overview

3.1.1 Problem Formulation

We follow the problem definition for procedure planning of instructional videos put forth by Chang *et al.* [9]: given an observation of the initial state v_{start} and a goal state v_{goal} , both are short video clips indicating different states of the real-world environment extracted from an instructional video, a model is required to plan a sequence of action steps $a_{1:T}$ to reach the indicated goal. Here, T is the planning horizon, inputting to the model, corresponding to the num-

ber of action steps in the sequence produced by the model so that the environment state can be transformed from v_{start} to v_{goal} . We use a_t to denote the action step at the timestamp t , and in the following, v_s and v_g are short for v_{start} and v_{goal} . Mathematically, the procedure planning problem is defined as $p(a_{1:T}|v_s, v_g)$ that denotes the conditional probability distribution of the action sequence $a_{1:T}$ given the initial visual observation v_{start} and the goal visual state v_{goal} .

3.1.2 Problem Decomposition

Considering the initial and final visual states are input, providing the most reliable information, we hypothesize that predicting the first and final action steps is more dependable than interpolating the intermediate ones, and consequently, an enhanced accuracy in predicting the first and final steps can lead to more effective procedure planning. Inspired by this hypothesis, we decompose the procedure planning problem into two sub-problems, as shown in Eq. 9:

$$p(\hat{a}_{1:T}|v_s, v_g) = p(\hat{a}_{2:T-1}|\hat{a}_1, \hat{a}_T) p(\hat{a}_1, \hat{a}_T|v_s, v_g), \quad (1)$$

where the first sub-problem is to identify the beginning step a_1 and the end step a_T , and the second sub-problem is to plan the intermediate action steps $a_{2:T-1}$ given a_1 and a_T . We use \hat{a}_t to denote *predicted* action step at timestamp t .

Our proposed problem decomposition in Eq. 9 bears resemblance with the problem formulation proposed by Li *et al.* [29]; they decompose procedure planning into $p(\hat{a}_{1:T}|v_s, v_g) = \prod_{t=2}^{T-1} p(\hat{a}_t|\hat{a}_1, \hat{a}_T) p(\hat{a}_1, \hat{a}_T|v_s, v_g)$. However, our formulation differs in its approach to modeling the second sub-problem. Specifically, we employ a conditioned projected diffusion model (ref. § 3.2) to jointly predict $a_{2:T-1}$ at once, whereas Li *et al.* [29] rely on Transformer decoders to predict each intermediate action independently. Furthermore, we integrate a probabilistic procedure knowledge graph (ref. § 3.2.2) to address the second sub-problem.

Tackling the second sub-problem is nontrivial even when armed with an oracle predictor for the first sub-problem. Procedure planning in real-life scenarios remains daunting because of the following **challenges**: (1) the presence of implicit temporal and causal constraints in the sequencing of steps, (2) the existence of numerous viable plans given an initial state and a goal state, and (3) the need to incorporate the real-life everyday knowledge both in task-sharing steps and in managing the inherent variability in transition probabilities between steps. Previous studies tackled these challenges by extensively harnessing detailed annotations in the datasets to augment input features or offer supervision signals (see Table 1). In contrast, we propose harnessing a Probabilistic Procedural Knowledge Graph (P²KG) which is extracted from the procedure plans in the training set. With the P²KG at our hand, we further decompose the procedure planning problem to reduce its complexity and learn

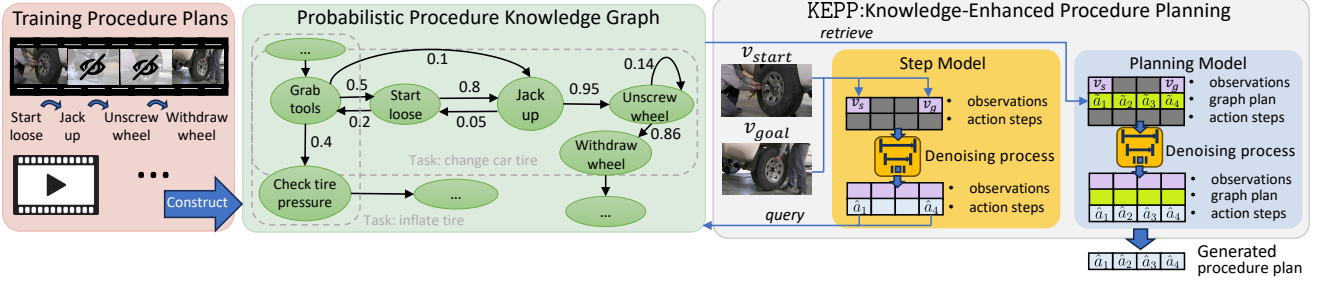


Figure 2. **Overview of our methodology.** We introduce KEPP, a Knowledge-Enhanced Procedure Planning system for instructional videos, leveraging a Probabilistic Procedural Knowledge Graph (P²KG). KEPP breaks down procedure planning into two parts: predicting initial and final steps from visual states, and crafting a procedure plan based on the procedural knowledge retrieved from P²KG, conditioned on the predicted first and last action steps. KEPP requires minimal annotations and enhances planning effectiveness

$f_\theta : (v_s, v_g, T) \rightarrow p(\hat{a}_{1:T} | v_s, v_g)$ as follows:

$$p(\hat{a}_{1:T} | v_s, v_g) = p(\hat{a}_{1:T} | \tilde{a}_{1:T}, v_s, v_g) p(\tilde{a}_{1:T} | \hat{a}_1, \hat{a}_T) p(\hat{a}_1, \hat{a}_T | v_s, v_g) \quad (2)$$

where f_θ denotes the machine learning model, and $\tilde{a}_{1:T}$ represents a graph path (i.e., a sequence of nodes) from P²KG. This retrieved graph path provides a valuable procedure plan recommendation aligned with the training domain, thus mitigating the complexity of procedure planning.

It is worth noting that the proposed approach to modeling procedure planning using Eq. 2 demands only a minimal level of supervision, merely relying on the ground truth training procedure plan; Eq. 2 circumvents the need for additional annotations. We describe details of our P²KG-enhanced approach in the following subsection.

3.2. KEPP: Knowledge-Enhanced Procedure Planning

We propose KEPP (Fig. 2) utilizing a probabilistic procedure knowledge graph extracted from the training set. We firstly identify the beginning and conclusion steps according to the input initial and goal states; and then, conditioned on these steps and the planning horizon T , we query the graph to retrieve relevant procedural knowledge for knowledge-enhanced procedure planning of instructional videos.

3.2.1 Identify Beginning and Conclusion Steps

Given v_{start} and v_{goal} as input, we adapt a Conditioned Projected Diffusion Model [50] (ref. supplementary material) to identify the first action step and the final step; we refer to this model as the ‘Step (Perception) Model’.

Standard Denoising Diffusion Probabilistic Model tackles data generation through a denoising Markov chain over variables $\{x_N \dots x_0\}$, starting with x_N as a Gaussian random distribution [22]. In the forward diffusion phase, Gaussian noise $\epsilon \sim \mathcal{N}(0, \mathbf{I})$ is progressively added to the initial, unaltered data x_0 , transforming it into a Gaussian ran-

dom distribution. Conversely, the reverse denoising process transforms Gaussian noise back into a sample. Denoising is parameterized by a learnable noise prediction model, and the learning objective is to learn the noise added to x_0 at each diffusion step. After training, the diffusion model generates data akin to x_0 by iteratively applying the denoising process, starting from random Gaussian noise.

Adopting Conditioned Projected Diffusion Model as the Step Model. For our step model, the distribution we aim to fit is the two-action sequence $[a_1, a_T]$, based on the visual initial and goal states, v_{start} and v_{goal} . These conditional visual states are concatenated with the actions along the action feature dimension, forming a multi-dimensional array:

$$\begin{bmatrix} v_s & 0 & \dots & 0 & v_g \\ a_1 & 0 & \dots & 0 & a_T \end{bmatrix} \quad (3)$$

where the array is zero-padded to have a length corresponds to the planning horizon T . During the denoising process, these conditional visual states can change, potentially misleading the learning process. To prevent this, a condition projection operation [50] is applied, ensuring the visual state and zero-padding dimensions remain unchanged (shaded below). The projection operation can be denoted as follows:

$$\begin{bmatrix} \hat{v}_1 & \hat{v}_2 & \dots & \hat{v}_{T-1} & \hat{v}_T \\ \hat{a}_1 & \hat{a}_2 & \dots & \hat{a}_{T-1} & \hat{a}_T \end{bmatrix} \xrightarrow{\text{Projection}} \begin{bmatrix} v_s & 0 & \dots & 0 & v_g \\ \hat{a}_1 & 0 & \dots & 0 & \hat{a}_T \end{bmatrix} \quad (4)$$

where \hat{v}_t denotes the predicted visual state dimensions at timestamp t within the planning horizon T .

3.2.2 Construct the Probabilistic Procedure Knowledge Graph (P²KG)

The Probabilistic Procedure Knowledge Graph [5] P²KG = (V, E, w) is a directed and weighted graph. In this structure, each step from the training set is represented as a node. During the graph construction process, we iterate over the training procedure plans, and for each direct step transition present in a plan, we add an edge from a_t to a_{t+1} if it does

not already exist in the graph; otherwise, we increase its existing frequency count by one. Eventually, this process results in a frequency-based Procedural Knowledge Graph (PKG) [58], which adeptly encapsulating the complexities of step sequencing in procedures and its potential variations, thereby addressing challenges (1) and (2) of procedure planning (ref. § 3.1.2). To further tackle challenge (3), this graph undergoes a transformation into a probabilistic format. In this transformed graph, the edges are not just connections but also signify the likelihoods of transitioning from one step to another. The weight of an edge from a_t to a_{t+1} is the count of transitions from action step a_t to a_{t+1} normalized by total count of a_t being executed [5]. The normalization converts the frequency-based weight into probability distribution and the sum of all out-going edges is one.

3.2.3 P²KG-Enhanced Procedure Planning

Retrieving Procedure Plan Recommendations from the P²KG. Humans use both previously-acquired knowledge and external knowledge when solving problems. The P²KG provides extensive procedural knowledge, serving as a comprehensive textbook, particularly beneficial for the planning model that requires advanced skills. To utilize this procedural knowledge, queries are made to the P²KG using the first (\hat{a}_1) and last (\hat{a}_T) actions predicted by the step model. The aim is to find graph paths no longer than T steps, starting from \hat{a}_1 and ending at \hat{a}_T .

This above process often results in multiple possible paths. To evaluate these paths, the probability of each is calculated by multiplying the probability weights of the edges along the path. For instance, the probability of a path $a_1 \rightarrow a_2 \rightarrow a_3$ is determined by the product $w_{a_1 \rightarrow a_2} \times w_{a_2 \rightarrow a_3}$. These paths are then ranked according to their probabilities, and the top R paths are selected as the recommended procedural plans from the P²KG, where R is predefined.

For paths shorter than T , padding is applied at any point in the middle of the sequence to explore all possible resultant paths. When R is greater than one, the top R paths are aggregated through linear weighting into a single path. This final path is then used as an additional input for the procedure planning model, thereby enhancing its decision-making process.

Adopting Conditioned Projected Diffusion Model as the Planning Model. For the planning model, the conditional visual states and the procedure plan recommendation from the P²KG are concatenated with the actions along the action feature dimension, forming a multi-dimensional array:

$$\begin{bmatrix} v_s & 0 & \dots & 0 & v_g \\ \tilde{a}_1 & \tilde{a}_2 & \dots & \tilde{a}_{T-1} & \tilde{a}_T \\ a_1 & a_2 & \dots & a_{T-1} & a_T \end{bmatrix} \quad (5)$$

The rest process is similar to the step model, except that the project operation guarantees that three specific aspects

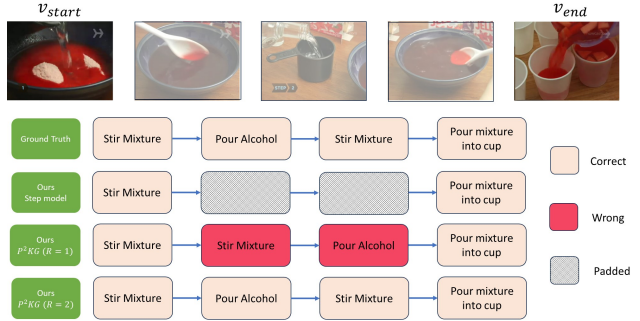


Figure 3. Qualitative analysis of the ‘Make Jello Shots’ task

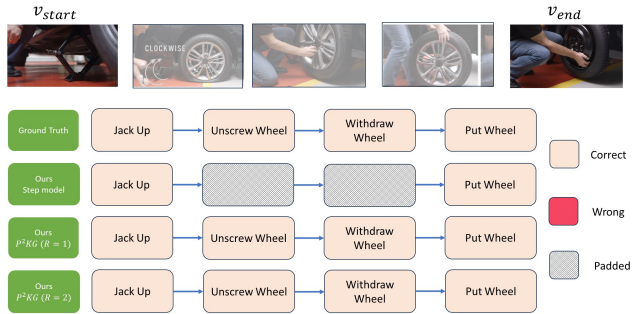


Figure 4. Qualitative analysis of the ‘Change a Tire’ task

remain unaltered—the dimensions of the the visual state, P²KG recommendation, and zero-padding.

4. Experiments

4.1. Evaluation Protocol

Datasets: In our evaluation, we employed datasets from three sources: CrossTask [59], COIN [48], and the Narrated Instructional Videos (NIV) [4]. The CrossTask dataset comprises 2,750 video clips, each representing one of 18 distinct tasks, and features an average of 7.6 actions per clip. The COIN dataset is more extensive, including 11,827 videos across 180 tasks, with an average of 3.6 actions per video. Lastly, the NIV dataset, though smaller in scale, includes 150 videos that capture 5 everyday tasks, with a higher density of actions, averaging 9.5 actions per video. All ablation studies and analyses were conducted on CrossTask.

Implementation Details: We use two Tesla A100 GPUs for all the experiments. We chose horizon $T \in \{3, 4, 5, 6\}$ and P²KG ($R=1$) condition for implementation. In some cases, we incorporate P²KG ($R=2$) and LLM conditions which are indicated in the respective tables. Throughout this study, the P²KG ($R=1$) is employed with a batch size of 256, unless explicitly stated otherwise. More implementation details are available in the supplementary material.

Evaluation Metrics: Our study employs mean intersection over union (mIoU), mean accuracy (mAcc), and suc-

Models	Required Annotations				$T = 3$			$T = 4$		
	step class	visual states	step text	task class	SR^\dagger	$mAcc^\dagger$	$mIoU^\dagger$	SR^\dagger	$mAcc^\dagger$	$mIoU^\dagger$
Random	✓				< 0.01	0.94	1.66	< 0.01	0.83	1.66
Retrieval-Based	✓				8.05	23.3	32.06	3.95	22.22	36.97
WLTD0 [16]	✓	✓			1.87	21.64	31.70	0.77	17.92	26.43
UAAA [1]	✓	✓			2.15	20.21	30.87	0.98	19.86	27.09
UPN [45]	✓	✓			2.89	24.39	31.56	1.19	21.59	27.85
DDN [9]	✓	✓			12.18	31.29	47.48	5.97	27.10	48.46
PlaTe [46]	✓	✓			16.00	36.17	65.91	14.00	35.29	55.36
Ext-GAIL wo Aug. [7]	✓	✓			18.01	43.86	57.16	-	-	-
Ext-GAIL [7]	✓	✓			21.27	49.46	61.70	16.41	43.05	60.93
P ³ IV ♣ [55]	✓		✓		23.34	49.96	73.89	13.40	44.16	70.01
PDPP ♣ [50]	✓			✓	26.38	55.62	59.34	18.69	52.44	62.38
E3P ♣ [49]	✓		✓	✓	26.40	53.02	74.05	16.49	48.00	70.16
SkipPlan [29] ♣	✓				28.85	61.18	74.98	15.56	55.64	70.30
Ours w/ P ² KG ($R=2$)	✓				22.60	48.76	53.57	13.90	45.79	55.00
Ours ♣ w/ P ² KG ($R=1$)	✓				33.34	61.36	64.14	20.38	55.54	64.03
Ours ♣ w/ P ² KG ($R=2$)	✓				33.38	60.79	63.89	21.02	56.08	64.15
PDPP ♣ † [50]	✓			✓	37.20	64.67	66.57	21.48	57.82	65.13
Ours ♣ † w/ P ² KG ($R=1$)	✓				38.12	64.74	67.15	24.15	59.05	66.64

Table 1. Performance of our method in comparison to existing baselines for CrossTask dataset. ♣ means that the input visual features are from the S3D network [34] pretrained on HowTo100M [33]; otherwise, precomputed features provided in CrossTask are used. † indicates the results are under the PDPP’s setting, while others are under the conventional setting

Models	$T = 5$	$T = 6$
DDN [9]	3.10	1.20
P ³ IV ♣ [55]	7.21	4.40
PDPP ♣ [50]	13.22	7.49
E3P ♣ [49]	8.96	5.76
SkipPlan ♣ [29]	8.55	5.12
Ours ($R=2$)	8.17	5.32
Ours ♣ ($R=1$)	13.25	8.09
Ours ♣ ($R=2$)	12.74	9.23
PDPP ♣ † [50]	13.45	8.41
Ours ♣ † ($R=1$)	14.20	9.27

Table 2. Success Rate (SR^\dagger) comparison to existing baselines for CrossTask dataset under longer horizons

cess rate (SR) as our evaluation metrics. mIoU evaluates the overlap between the predicted actions with the ground-truth actions using IoU by regarding them as two action sets. mAcc is quantified as the average of the precise correspondences between the predicted actions and their respective ground truth counterparts at corresponding time steps. Thus, mAcc counts the order of actions, and is stricter than mIoU. **SR is the most stringent metric**, considering a sequence to be successful solely if it exhibits a perfect match with the ground truth action sequence throughout.

Baselines: We compare our model with widely used state-

of-the-art methods: WLTD0 [16], UAAA [1], UPN [45], DDN [9], PlaTe [46], Ext-GAIL [7], P³IV [55], PDPP [50], SkipPlan [29], and E3P [49]. More details of these methods are available in the supplementary material. Compared to other models, PDPP uses a different experimental setting. In PDPP, authors set the window after the start time of a_1 and before the end time of a_T , contrary to the standard practice of setting a 2-second window around the start and end time (*ref.* [9]). We conduct the experiments on both PDPP’s proposed setting and the conventional setting.

4.2. Comparison with the State of the Art (SOTA)

CrossTask (short horizon): We evaluate on CrossTask for short horizons ($T = 3$ and $T = 4$). According to the results shown in Table 1, our proposed method outperforms the PDPP in PDPP’s setting in every evaluation metric. More than 0.9% and 2% improvement in success rate in $T = 3$ and $T = 4$ respectively. In the conventional setting, our method with both P²KG ($R=1$) and P²KG ($R=2$) conditions outperform the success rate values by a significant margin compared to other baselines. P²KG ($R=2$) slightly outperforms P²KG ($R=1$), indicating potential benefits of incorporating more procedural knowledge from the P²KG.

CrossTask (long horizon): We use long-horizon predictions for $T = 5$ and $T = 6$ for further evaluating our model as shown in Table 2. In PDPP’s setting (†), our method improves the success rate in both $T = 5$ and $T = 6$. In

the conventional setting, our method utilizing P²KG ($R=1$) demonstrates the highest SR value for $T = 5$, and for a longer horizon at $T = 6$, our method delivers superior performance for P²KG ($R=2$). Our method performs well under the challenging scenario of a long planning horizon.

NIV and COIN: Evaluations of our method on other datasets are shown in Table 3 and Table 4. On NIV, ours achieves the best result under the mIoU metric with $T=3$, and under both the SR and mIoU metrics with $T=4$. Our method does not rank as the top performer on COIN. The likely reason is that the COIN dataset features just an average of 3.6 actions per video—a scenario that does not necessitate advanced procedural (sequence-level) knowledge. Furthermore, the dataset’s extensive collection of over 11k videos provides a substantial resource for baselines to learn basic procedural knowledge. The results on COIN ($T=4$) is available in the supplementary material.

Models	NIV ($T=3$)			NIV ($T=4$)		
	SR^\uparrow	$mAcc^\uparrow$	$mIoU^\uparrow$	SR^\uparrow	$mAcc^\uparrow$	$mIoU^\uparrow$
Random	2.21	4.07	6.09	1.12	2.73	5.84
DDN [9]	18.41	32.54	56.56	15.97	27.09	53.84
Ext-GAIL [7]	22.11	42.20	65.93	19.91	36.31	53.84
P ³ IV [55]	24.68	49.01	74.29	20.14	38.36	67.29
E3P [49]	26.05	51.24	75.81	21.37	41.96	74.90
Ours	24.44	43.46	86.67	22.71	41.59	91.49

Table 3. Performance of baselines and ours for NIV dataset

Models	COIN		
	SR^\uparrow	$mAcc^\uparrow$	$mIoU^\uparrow$
($T=3$)			
Random	< 0.01	< 0.01	2.47
Retrieval	4.38	17.40	32.06
DDN [9]	13.9	20.19	64.78
Ext-GAIL [7]	-	-	-
P ³ IV [55]	15.4	21.67	76.31
E3P [49]	19.57	31.42	84.95
SkipPlan [29]	23.65	47.12	78.44
Ours	20.25	39.87	51.72

Table 4. Performance of baselines and ours for COIN dataset

4.3. Ablation Studies

Ablation on the probabilistic procedure knowledge graph. We analyze the role of P²KG in improving the performance of our proposed method. Table 5 shows the results which clearly demonstrate that using P²KG conditions improves the performance significantly for every T value. Especially when $T = 4$, success rate (SR) improves more than 3% and mean IoU improves more than 2%.

Plan recommendations provided by probabilistic procedure knowledge graph v.s. LLM. We recognize the recent trend of utilizing LLMs to enhance action anticipation [56] or planning in other realms [3, 27, 28, 42]. In Table 6, we compare the results between using P²KG v.s. using LLM

(‘llama-2-13b-chat’) to generate the plan recommendations. By looking at Table 6, we can confirm that using the P²KG recommendation gives more accurate results than just using the LLM generated recommendation.

Probabilistic procedure knowledge graph (P²KG) v.s. Frequency-based procedure knowledge graph (PKG).

The probabilistic procedure knowledge graph uses out-edge normalization to encode step transition probabilities (§ 3.2.2), while the frequency-based procedure knowledge graph uses min-max normalization over the frequency counts throughout the graph. In both cases, the planning model only uses 1 procedure plan recommendation from the graph as condition in our experimental analysis. By looking at the results shown in Table 7, it is evident that the probabilistic procedure knowledge graph outperforms the frequency-based procedure knowledge graph.

Effect of utilizing predicted steps for input conditions to train the procedure planing model.

Our proposed problem decomposition allows training the planning model with ground truth (GT) first and last steps. We experiment with two ways to train the planning model. Method 1 uses the predicted start and end steps (\hat{a}_1 and \hat{a}_T) as input to generate P²KG conditions and use them to train the planning model. Method 2 is where we augment the predicted start and end steps using the GT start and end steps (a_1 and a_T) by generating 3 more data samples as follows: $[\hat{a}_1, a_T]$, $[a_1, \hat{a}_T]$, and $[a_1, a_T]$. Then we generate P²KG conditions for each data and train the model. From the results shown in Table 8, we can see the method without GT data augmentation shows better results. This suggests that leveraging ground truth data during training can lead to worse performance during testing. While the step model does not consistently yield flawless predictions, this experiment validates the utility of using its predicted steps to train the planning model within our proposed problem decomposition.

4.4. Analyses

Qualitative results. In Figure 3 and Figure 4, we present qualitative examples of our proposed method. Intermediate steps are padded in the step model because it only predicts the start and end actions. In the ‘make jello shot’ task shown in Figure 3, the model gives a wrong prediction in the intermediate steps when using P²KG ($R=1$) condition. However, it predicts correctly when using P²KG ($R=2$) conditions. In the ‘change a tire’ task shown in Figure 4, the model is able to predict all the intermediate steps in given conditions.

Visualizations of the probabilistic procedure knowledge graph. In Figure 5, We show a sub-graph from our probabilistic procedure knowledge graph. This graph is drawn around the ‘jack up’ node up to the depth of 2 nodes.

Visualizations of the expert trajectories. Figure 6 illustrates the steps involved in completing the ‘make jello shots’ task, along with their transitions to other steps within the en-

Model	T=3			T=4			T=5			T=6		
	SR	mAcc	mIoU	SR	mAcc	mIoU	SR	mAcc	mIoU	SR	mAcc	mIoU
w.o P ² KG conditions †	35.69	63.91	66.04	20.52	57.47	64.39	12.8	53.44	64.01	8.15	50.45	64.13
Ours †	38.12	64.74	67.15	24.15	59.05	66.64	14.20	53.84	65.56	9.27	50.22	65.97

Table 5. Performance of our method with and without P²KG conditions on CrossTask ♣ dataset

Model ($T=6$, CrossTask ♣)	SR	mAcc	mIoU
Ours with P ² KG ($R=1$)			
PDPP setting	9.27	50.22	65.97
Conventional setting	8.09	50.80	65.39
1 LLM condition			
PDPP setting	7.74	50.28	64.05
Conventional setting	7.21	49.68	63.89
P ² KG ($R=1$) and 1 LLM condition			
PDPP setting	8.81	49.97	65.22
Conventional setting	8.20	51.46	64.30

Table 6. Performance of the plan recommendations provided by the probabilistic procedure knowledge graph v.s. LLM.

Models	SR	mAcc	mIoU
Frequency graph	7.66	48.61	64.21
Probabilistic graph	8.09	50.80	65.40

Table 7. Comparison of the performance between probabilistic procedure knowledge graph v.s. frequency-based procedure knowledge graph for $T=6$ on CrossTask ♣ dataset

Condition	SR	mAcc	mIoU
without GT data aug.	38.12	64.74	67.15
with GT data aug.	32.45	62.42	62.80

Table 8. Effect of different input conditions for performance on CrossTask ♣ dataset ($T=3$) in PDPP’s setting

Models	T=3		T=4		T=5		T=6	
	\hat{a}_1	\hat{a}_T	\hat{a}_1	\hat{a}_T	\hat{a}_1	\hat{a}_T	\hat{a}_1	\hat{a}_T
Ours	53.69	50.60	55.56	52.51	55.58	51.81	57.09	51.92
Ours ♣	71.42	63.32	72.98	63.37	72.42	63.29	63.82	59.96

Table 9. The step model’s start and end step prediction accuracies on the CrossTask dataset

tire training data. This figure demonstrates that our P²KG encodes diverse sequencing possibilities for steps and also captures task-sharing steps across the entire training domain. For instance, ‘pour water’ is a step in ‘make jello shots’ task, but it can also be part of other tasks, leading to a step transition from ‘pour water’ to ‘add fish.’ This structure allows models to leverage rich procedural knowledge.

Results for the step model. Table 9 presents the results of the step model, indicating potential areas for enhancement to elevate the planning performance.

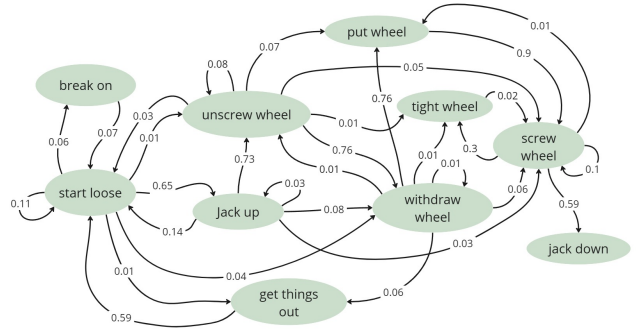


Figure 5. Example of a sub-graph in our probabilistic procedure knowledge graph (P²KG) for CrossTask dataset. This graph effectively encapsulates real-world knowledge of distinct transition probabilities between steps, e.g., the probability of transitioning from ‘start loose’ to ‘jack up’ is 0.65, in contrast to a mere 0.14 for the reverse transition—the P²KG reflects the common real-life practice where loosening the lug nuts before jacking up the car leads to a safer and more efficient tire change.

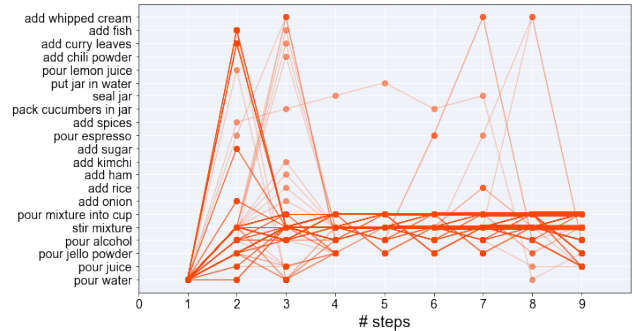


Figure 6. Expert trajectories of the ‘Make Jello Shots’ task, involving task-sharing steps and thus out-of-task step transitions. Thicker lines indicate paths that are more frequently visited

5. Conclusion

We focus on the formulation of procedural plans from an AI agent in the realm of instructional videos. We propose to enhance the agent’s capabilities by incorporating procedural knowledge. This knowledge is gleaned from the training procedure plans, enabling the agent to adeptly handle the intricacies of step sequencing and its variations. We term this innovative approach KEPP (Knowledge-Enhanced Procedure Planning). KEPP employs a probabilistic procedural knowledge graph, sourced from the training domain, effectively serving as a ‘textbook’ for procedure planning. Experiments conducted on three datasets demonstrate that KEPP delivers top-tier performance while necessitating only a minimal amount of supervision.

References

- [1] Yazan Abu Farha and Juergen Gall. Uncertainty-aware anticipation of activities. In *Proceedings of the IEEE/CVF International Conference on Computer Vision Workshops*, pages 0–0, 2019. 6, 7
- [2] Triantafyllos Afouras, Effrosyni Mavroudi, Tushar Nagarajan, Huiyu Wang, and Lorenzo Torresani. Ht-step: Aligning instructional articles with how-to videos. In *Thirty-seventh Conference on Neural Information Processing Systems Datasets and Benchmarks Track*, 2023. 2
- [3] Anurag Ajay, Seungwook Han, Yilun Du, Shaung Li, Abhi Gupta, Tommi Jaakkola, Josh Tenenbaum, Leslie Kaelbling, Akash Srivastava, and Pulkit Agrawal. Compositional foundation models for hierarchical planning. *arXiv preprint arXiv:2309.08587*, 2023. 7
- [4] Jean-Baptiste Alayrac, Piotr Bojanowski, Nishant Agrawal, Josef Sivic, Ivan Laptev, and Simon Lacoste-Julien. Unsupervised learning from narrated instruction videos. In *Proceedings of the IEEE Conference on Computer Vision and Pattern Recognition*, pages 4575–4583, 2016. 5
- [5] Kumar Ashutosh, Santhosh Kumar Ramakrishnan, Triantafyllos Afouras, and Kristen Grauman. Video-mined task graphs for keystone recognition in instructional videos. *arXiv preprint arXiv:2307.08763*, 2023. 2, 4, 5
- [6] Anonymous authors. Active procedure planning with uncertainty-awareness in instructional videos, 2023. Under review as a conference paper at ICLR 2024. <https://openreview.net/pdf?id=JDd46WodYf>. 1
- [7] Jing Bi, Jiebo Luo, and Chenliang Xu. Procedure planning in instructional videos via contextual modeling and model-based policy learning. In *Proceedings of the IEEE/CVF International Conference on Computer Vision*, pages 15611–15620, 2021. 1, 2, 6, 7
- [8] Faeze Brahman, Chandra Bhagavatula, Valentina Pyatkin, Jena D Hwang, Xiang Lorraine Li, Hirona J Arai, Soumya Sanyal, Keisuke Sakaguchi, Xiang Ren, and Yejin Choi. Plasma: Making small language models better procedural knowledge models for (counterfactual) planning. *arXiv preprint arXiv:2305.19472*, 2023. 2
- [9] Chien-Yi Chang, De-An Huang, Danfei Xu, Ehsan Adeli, Li Fei-Fei, and Juan Carlos Nieves. Procedure planning in instructional videos. In *European Conference on Computer Vision*, pages 334–350. Springer, 2020. 1, 2, 3, 6, 7
- [10] Brian Chen, Nina Shvetsova, Andrew Rouditchenko, Daniel Kondermann, Samuel Thomas, Shih-Fu Chang, Rogerio Feris, James Glass, and Hilde Kuehne. What, when, and where?—self-supervised spatio-temporal grounding in untrimmed multi-action videos from narrated instructions. *arXiv preprint arXiv:2303.16990*, 2023. 2
- [11] Sixun Dong, Huazhang Hu, Dongze Lian, Weixin Luo, Yicheng Qian, and Shenghua Gao. Weakly supervised video representation learning with unaligned text for sequential videos. In *Proceedings of the IEEE/CVF Conference on Computer Vision and Pattern Recognition*, pages 2437–2447, 2023. 2
- [12] Hazel Doughty, Ivan Laptev, Walterio Mayol-Cuevas, and Dima Damen. Action modifiers: Learning from adverbs in instructional videos. In *Proceedings of the IEEE/CVF Conference on Computer Vision and Pattern Recognition*, pages 868–878, 2020. 2
- [13] Yilun Du, Mengjiao Yang, Pete Florence, Fei Xia, Ayzaan Wahid, Brian Ichter, Pierre Sermanet, Tianhe Yu, Pieter Abbeel, Joshua B Tenenbaum, et al. Video language planning. *arXiv preprint arXiv:2310.10625*, 2023. 1, 2
- [14] Nikita Dvornik, Isma Hadji, Hai Pham, Dhaivat Bhatt, Brais Martinez, Afsaneh Fazly, and Allan D Jepson. Flow graph to video grounding for weakly-supervised multi-step localization. In *European Conference on Computer Vision*, pages 319–335. Springer, 2022. 2
- [15] Nikita Dvornik, Isma Hadji, Ran Zhang, Konstantinos G Derpanis, Richard P Wildes, and Allan D Jepson. Step-former: Self-supervised step discovery and localization in instructional videos. In *Proceedings of the IEEE/CVF Conference on Computer Vision and Pattern Recognition*, pages 18952–18961, 2023. 2
- [16] Kiana Ehsani, Hessam Bagherinezhad, Joseph Redmon, Roozbeh Mottaghi, and Ali Farhadi. Who let the dogs out? modeling dog behavior from visual data. In *Proceedings of the IEEE Conference on Computer Vision and Pattern Recognition*, pages 4051–4060, 2018. 6, 7
- [17] Sophie Fischer, Carlos Gemmell, Iain Mackie, and Jeffrey Dalton. Vilt: Video instructions linking for complex tasks. In *Proceedings of the 2nd International Workshop on Interactive Multimedia Retrieval*, pages 41–47, 2022. 2
- [18] Kevin Flanagan, Dima Damen, and Michael Wray. Learning temporal sentence grounding from narrated egovideos. *arXiv preprint arXiv:2310.17395*, 2023. 2
- [19] Daniel Fried, Jean-Baptiste Alayrac, Phil Blunsom, Chris Dyer, Stephen Clark, and Aida Nematzadeh. Learning to segment actions from observation and narration. *arXiv preprint arXiv:2005.03684*, 2020. 2
- [20] Chuang Gan, Siyuan Zhou, Jeremy Schwartz, Seth Alter, Abhishek Bhandwadar, Dan Gutfreund, Daniel LK Yamins, James J DiCarlo, Josh McDermott, Antonio Torralba, et al. The threedworld transport challenge: A visually guided task-and-motion planning benchmark for physically realistic embodied ai. *arXiv preprint arXiv:2103.14025*, 2021. 2
- [21] Reza Ghoddoosian, Isht Dwivedi, Nakul Agarwal, and Behzad Dariush. Weakly-supervised action segmentation and unseen error detection in anomalous instructional videos. In *Proceedings of the IEEE/CVF International Conference on Computer Vision*, pages 10128–10138, 2023. 2
- [22] Jonathan Ho, Ajay Jain, and Pieter Abbeel. Denoising diffusion probabilistic models. *Advances in neural information processing systems*, 33:6840–6851, 2020. 4, 5
- [23] Guyue Hu, Bin He, and Hanwang Zhang. Compositional prompting video-language models to understand procedure in instructional videos. *Machine Intelligence Research*, 20(2):249–262, 2023. 2
- [24] De-An Huang, Joseph J Lim, Li Fei-Fei, and Juan Carlos Nieves. Unsupervised visual-linguistic reference resolution in instructional videos. In *Proceedings of the IEEE Conference on Computer Vision and Pattern Recognition*, pages 2183–2192, 2017. 2

- [25] De-An Huang, Shyamal Buch, Lucio Dery, Animesh Garg, Li Fei-Fei, and Juan Carlos Nieves. Finding” it”: Weakly-supervised reference-aware visual grounding in instructional videos. In *Proceedings of the IEEE Conference on Computer Vision and Pattern Recognition*, pages 5948–5957, 2018. [2](#)
- [26] Gabriel Huang, Bo Pang, Zhenhai Zhu, Clara Rivera, and Radu Soricut. Multimodal pretraining for dense video captioning. *arXiv preprint arXiv:2011.11760*, 2020. [2](#)
- [27] Wenlong Huang, Pieter Abbeel, Deepak Pathak, and Igor Mordatch. Language models as zero-shot planners: Extracting actionable knowledge for embodied agents. In *International Conference on Machine Learning*, pages 9118–9147. PMLR, 2022. [2](#), [7](#)
- [28] Wenlong Huang, Fei Xia, Ted Xiao, Harris Chan, Jacky Liang, Pete Florence, Andy Zeng, Jonathan Tompson, Igor Mordatch, Yevgen Chebotar, et al. Inner monologue: Embodied reasoning through planning with language models. *arXiv preprint arXiv:2207.05608*, 2022. [2](#), [7](#)
- [29] Zhiheng Li, Wenjia Geng, Muheng Li, Lei Chen, Yansong Tang, Jiwen Lu, and Jie Zhou. Skip-plan: Procedure planning in instructional videos via condensed action space learning. In *Proceedings of the IEEE/CVF International Conference on Computer Vision*, pages 10297–10306, 2023. [2](#), [3](#), [6](#), [7](#), [1](#), [8](#)
- [30] Yujie Lu, Weixi Feng, Wanrong Zhu, Wenda Xu, Xin Eric Wang, Miguel Eckstein, and William Yang Wang. Neuro-symbolic procedural planning with commonsense prompting. In *The Eleventh International Conference on Learning Representations*, 2022. [2](#)
- [31] Yujie Lu, Pan Lu, Zhiyu Chen, Wanrong Zhu, Xin Eric Wang, and William Yang Wang. Multimodal procedural planning via dual text-image prompting. *arXiv preprint arXiv:2305.01795*, 2023. [2](#)
- [32] Effrosyni Mavroudi, Triantafyllos Afouras, and Lorenzo Torresani. Learning to ground instructional articles in videos through narrations. *arXiv preprint arXiv:2306.03802*, 2023. [2](#)
- [33] Antoine Miech, Dimitri Zhukov, Jean-Baptiste Alayrac, Makarand Tapaswi, Ivan Laptev, and Josef Sivic. Howto100m: Learning a text-video embedding by watching hundred million narrated video clips. In *Proceedings of the IEEE/CVF international conference on computer vision*, pages 2630–2640, 2019. [1](#), [6](#)
- [34] Antoine Miech, Jean-Baptiste Alayrac, Lucas Smaira, Ivan Laptev, Josef Sivic, and Andrew Zisserman. End-to-end learning of visual representations from uncurated instructional videos. In *Proceedings of the IEEE/CVF Conference on Computer Vision and Pattern Recognition*, pages 9879–9889, 2020. [2](#), [6](#), [1](#)
- [35] Davide Moltisanti, Frank Keller, Hakan Bilen, and Laura Sevilla-Lara. Learning action changes by measuring verb-adverb textual relationships. In *Proceedings of the IEEE/CVF Conference on Computer Vision and Pattern Recognition*, pages 23110–23118, 2023. [2](#)
- [36] Medhini Narasimhan, Arsha Nagrani, Chen Sun, Michael Rubinstein, Trevor Darrell, Anna Rohrbach, and Cordelia Schmid. Tl; dw? summarizing instructional videos with task relevance and cross-modal saliency. In *European Conference on Computer Vision*, pages 540–557. Springer, 2022. [2](#)
- [37] Megha Nawhal, Akash Abdu Jyothi, and Greg Mori. Rethinking learning approaches for long-term action anticipation. In *European Conference on Computer Vision*, pages 558–576. Springer, 2022. [2](#)
- [38] Fadime Sener, Rishabh Saraf, and Angela Yao. Transferring knowledge from text to video: Zero-shot anticipation for procedural actions. *IEEE Transactions on Pattern Analysis and Machine Intelligence*, 2022. [2](#)
- [39] Anshul Shah, Benjamin Lundell, Harpreet Sawhney, and Rama Chellappa. Steps: Self-supervised key step extraction from unlabeled procedural videos. *arXiv preprint arXiv:2301.00794*, 2023. [2](#)
- [40] Yuhan Shen, Lu Wang, and Ehsan Elhamifar. Learning to segment actions from visual and language instructions via differentiable weak sequence alignment. In *Proceedings of the IEEE/CVF Conference on Computer Vision and Pattern Recognition*, pages 10156–10165, 2021. [2](#)
- [41] Mohit Shridhar, Jesse Thomason, Daniel Gordon, Yonatan Bisk, Winson Han, Roozbeh Mottaghi, Luke Zettlemoyer, and Dieter Fox. Alfred: A benchmark for interpreting grounded instructions for everyday tasks. In *Proceedings of the IEEE/CVF conference on computer vision and pattern recognition*, pages 10740–10749, 2020. [2](#)
- [42] Ishika Singh, Valts Blukis, Arsalan Mousavian, Ankit Goyal, Danfei Xu, Jonathan Tremblay, Dieter Fox, Jesse Thomason, and Animesh Garg. Progprompt: Generating situated robot task plans using large language models. In *2023 IEEE International Conference on Robotics and Automation (ICRA)*, pages 11523–11530. IEEE, 2023. [2](#), [7](#)
- [43] Yale Song, Gene Byrne, Tushar Nagarajan, Huiyu Wang, Miguel Martin, and Lorenzo Torresani. Ego4d goal-step: Toward hierarchical understanding of procedural activities. In *Thirty-seventh Conference on Neural Information Processing Systems Datasets and Benchmarks Track*, 2023. [2](#)
- [44] Tomáš Souček, Jean-Baptiste Alayrac, Antoine Miech, Ivan Laptev, and Josef Sivic. Look for the change: Learning object states and state-modifying actions from untrimmed web videos. In *Proceedings of the IEEE/CVF Conference on Computer Vision and Pattern Recognition*, pages 13956–13966, 2022. [2](#)
- [45] Aravind Srinivas, Allan Jabri, Pieter Abbeel, Sergey Levine, and Chelsea Finn. Universal planning networks: Learning generalizable representations for visuomotor control. In *International Conference on Machine Learning*, pages 4732–4741. PMLR, 2018. [6](#), [7](#)
- [46] Jiankai Sun, De-An Huang, Bo Lu, Yun-Hui Liu, Bolei Zhou, and Animesh Garg. Plate: Visually-grounded planning with transformers in procedural tasks. *IEEE Robotics and Automation Letters*, 7(2):4924–4930, 2022. [1](#), [2](#), [6](#), [7](#)
- [47] Reuben Tan, Bryan Plummer, Kate Saenko, Hailin Jin, and Bryan Russell. Look at what i’m doing: Self-supervised spatial grounding of narrations in instructional videos. *Advances in Neural Information Processing Systems*, 34:14476–14487, 2021. [2](#)
- [48] Yansong Tang, Dajun Ding, Yongming Rao, Yu Zheng, Danyang Zhang, Lili Zhao, Jiwen Lu, and Jie Zhou. Coin:

- A large-scale dataset for comprehensive instructional video analysis. In *Proceedings of the IEEE/CVF Conference on Computer Vision and Pattern Recognition*, pages 1207–1216, 2019. [5](#)
- [49] An-Lan Wang, Kun-Yu Lin, Jia-Run Du, Jingke Meng, and Wei-Shi Zheng. Event-guided procedure planning from instructional videos with text supervision. In *Proceedings of the IEEE/CVF International Conference on Computer Vision*, pages 13565–13575, 2023. [1](#), [2](#), [3](#), [6](#), [7](#), [8](#)
- [50] Hanlin Wang, Yilu Wu, Sheng Guo, and Limin Wang. Pdp: Projected diffusion for procedure planning in instructional videos. In *Proceedings of the IEEE/CVF Conference on Computer Vision and Pattern Recognition*, pages 14836–14845, 2023. [1](#), [2](#), [3](#), [4](#), [6](#), [5](#), [8](#)
- [51] Frank F Xu, Lei Ji, Botian Shi, Junyi Du, Graham Neubig, Yonatan Bisk, and Nan Duan. A benchmark for structured procedural knowledge extraction from cooking videos. *arXiv preprint arXiv:2005.00706*, 2020. [2](#)
- [52] Yue Yang, Joongwon Kim, Artemis Panagopoulou, Mark Yatskar, and Chris Callison-Burch. Induce, edit, retrieve: Language grounded multimodal schema for instructional video retrieval. *arXiv preprint arXiv:2111.09276*, 2021. [2](#)
- [53] Abhay Zala, Jaemin Cho, Satwik Kottur, Xilun Chen, Barlas Oguz, Yashar Mehdad, and Mohit Bansal. Hierarchical video-moment retrieval and step-captioning. In *Proceedings of the IEEE/CVF Conference on Computer Vision and Pattern Recognition*, pages 23056–23065, 2023. [2](#)
- [54] Jiahao Zhang, Anoop Cherian, Yanbin Liu, Yizhak Ben-Shabat, Cristian Rodriguez, and Stephen Gould. Aligning step-by-step instructional diagrams to video demonstrations. In *Proceedings of the IEEE/CVF Conference on Computer Vision and Pattern Recognition*, pages 2483–2492, 2023. [2](#)
- [55] He Zhao, Isma Hadji, Nikita Dvornik, Konstantinos G Derpanis, Richard P Wildes, and Allan D Jepson. P3iv: Probabilistic procedure planning from instructional videos with weak supervision. In *Proceedings of the IEEE/CVF Conference on Computer Vision and Pattern Recognition*, pages 2938–2948, 2022. [1](#), [2](#), [3](#), [6](#), [7](#), [8](#)
- [56] Qi Zhao, Ce Zhang, Shijie Wang, Changcheng Fu, Nakul Agarwal, Kwonjoon Lee, and Chen Sun. Antgpt: Can large language models help long-term action anticipation from videos? *arXiv preprint arXiv:2307.16368*, 2023. [7](#)
- [57] Yiwu Zhong, Licheng Yu, Yang Bai, Shangwen Li, Xueting Yan, and Yin Li. Learning procedure-aware video representation from instructional videos and their narrations. In *Proceedings of the IEEE/CVF Conference on Computer Vision and Pattern Recognition*, pages 14825–14835, 2023. [2](#)
- [58] Honglu Zhou, Roberto Martín-Martín, Mubbasir Kapadia, Silvio Savarese, and Juan Carlos Niebles. Procedure-aware pretraining for instructional video understanding. In *Proceedings of the IEEE/CVF Conference on Computer Vision and Pattern Recognition*, pages 10727–10738, 2023. [2](#), [5](#)
- [59] Dimitri Zhukov, Jean-Baptiste Alayrac, Ramazan Gokberk Cinbis, David Fouhey, Ivan Laptev, and Josef Sivic. Cross-task weakly supervised learning from instructional videos. In *Proceedings of the IEEE/CVF Conference on Computer Vision and Pattern Recognition*, pages 3537–3545, 2019. [1](#), [2](#), [5](#)

Why Not Use Your Textbook? Knowledge-Enhanced Procedure Planning of Instructional Videos

Supplementary Material

Unless otherwise mentioned, all the results and analysis are obtained for the CrossTask dataset with input visual features from the S3D network [34] pretrained on HowTo100M [33]. We organize the Supplementary Materials as follows:

- A. Further Experimental Results**
 - A.1 Additional Results on COIN and NIV**
 - A.2 Parameter Sensitivity Analysis**
- B. More Thorough Analysis**
 - B.1 More Qualitative Results**
 - B.2 More Visualizations of the P²KG**
 - B.3 Training Efficiency**
 - B.4 Analysis by the Step Transition Heatmap**
 - B.5 Limitations and Failure Cases**
- C. Method and Implementation Details**
 - C.1 Diffusion Model Details**
 - C.2 Implementation of KEPP**
 - C.3 Implementation of Ablations**
 - C.4 Baselines**

A. Further Experimental Results

A.1 Additional Results on COIN and NIV

COIN. We present the performance of our method in comparison to several baseline approaches on the COIN dataset across different planning horizons in Table S.1. While the results demonstrate that our method outperforms the majority of previous literature, it does not secure the top position when considering small planning horizons ($T=3$ or $T=4$) for the COIN dataset. This can be attributed to the fact that the COIN dataset typically consists of only 3.6 actions per video on average, a scenario where advanced sequence-level procedural knowledge is not essential. The advantage of our method becomes increasingly pronounced as the planning horizon expands. With a larger planning horizon ($T=5$), our method significantly outperforms the previous state-of-the-art (SOTA) methods, achieving a performance gain of 6.16 on the most strict metric, Success Rate (SR), compared to SkipPlan [29]. Our method’s utilization of plan recommendations from the Probabilistic Procedure Knowledge Graph (P²KG) effectively reduces the complexity of long-horizon planning.

NIV. Previous works did not provide results for the NIV dataset concerning long-horizon procedural planning; in Table S.2, we evaluate our model’s performance in comparison to the PDPP model [50] specifically on the NIV dataset

for long-horizon procedural planning ($T=5$ or $T=6$). (For results regarding short-horizon planning, please refer to Table 3 in the main paper.) Our model demonstrates superior performance in terms of the SR, mAcc, and mIoU metrics.

A.2 Parameter Sensitivity Analysis on the Number of Plan Recommendations

Our proposed method involves querying a probabilistic procedure knowledge graph; this process extracts the most probable graph paths, which have specified start and end steps. These paths are subsequently considered as recommended procedural plans and are employed as additional input conditions for the model, with the aim of improving its overall performance in procedure planning. Consequently, the number of plan recommendations, denoted as R in the main paper, emerges as a novel hyper-parameter in our methodology.

We have conducted a parameter sensitivity analysis to examine the effect of the number of paths selected from the probabilistic procedure knowledge graph to be given as conditions to the planning model on the procedure planning performance. Table S.3 displays the parameter sensitivity of our method with respect to R on the CrossTask dataset for the planning horizon $T=4$. To maintain simplicity in implementation, in cases where R exceeds one, we aggregate the features of the top R graph paths through a linear weighting process (i.e., weighted summation). This results in consistent feature dimensions compared to when $R=1$. The weighting scheme is as follows:

$$\begin{aligned} R = 1 &\rightarrow \text{weights} : 1 \\ R = 2 &\rightarrow \text{weights} : \frac{2}{3}, \frac{1}{3} \\ R = 3 &\rightarrow \text{weights} : \frac{3}{5}, \frac{1}{5}, \frac{1}{5} \\ R = 4 &\rightarrow \text{weights} : \frac{4}{7}, \frac{1}{7}, \frac{1}{7}, \frac{1}{7} \\ R = 5 &\rightarrow \text{weights} : \frac{5}{9}, \frac{1}{9}, \frac{1}{9}, \frac{1}{9}, \frac{1}{9} \end{aligned}$$

where the weights of the graph paths, starting with the most probable one, are provided above. The weights are empirically determined to emphasize the top one probable path by assigning it greater weight, and equal weights are distributed among the remaining graph paths.

Our method, with $R=2$, achieves the best results in SR and mIoU (see Table S.3). In general, performance of our method initially increases and then decreases as R continues to increase. The reason for larger values of R yielding lower SR is attributed to the influence of less prominent paths being included in the conditions given to the planning model. Further tuning of the weighting scheme could potentially yield even more superior results which we leave

Models	COIN ($T=3$)			COIN ($T=4$)			COIN ($T=5$)		
	SR^\uparrow	$mAcc^\uparrow$	$mIoU^\uparrow$	SR^\uparrow	$mAcc^\uparrow$	$mIoU^\uparrow$	SR^\uparrow	$mAcc^\uparrow$	$mIoU^\uparrow$
Random	< 0.01	< 0.01	2.47	< 0.01	< 0.01	2.32	-	-	-
Retrieval	4.38	17.40	32.06	2.71	14.29	36.97	-	-	-
DDN [9]	13.9	20.19	64.78	11.13	17.71	68.06	-	-	-
P ³ IV [55]	15.4	21.67	76.31	11.32	18.85	70.53	4.27	10.81	68.81
E3P [49]	19.57	31.42	84.95	13.59	26.72	84.72	-	-	-
SkipPlan [29]	23.65	47.12	78.44	16.04	43.19	77.07	9.90	38.99	76.93
Ours ($R=2$)	20.25	39.87	51.72	15.63	39.53	53.27	16.06	40.72	56.15

Table S.1. **Performance of baselines and ours on the COIN dataset.** Our method excels at handling challenging planning scenarios that demand longer planning horizons (T); with $T=5$, ours achieves a performance gain of 6.16 on the most strict metric, Success Rate (SR)

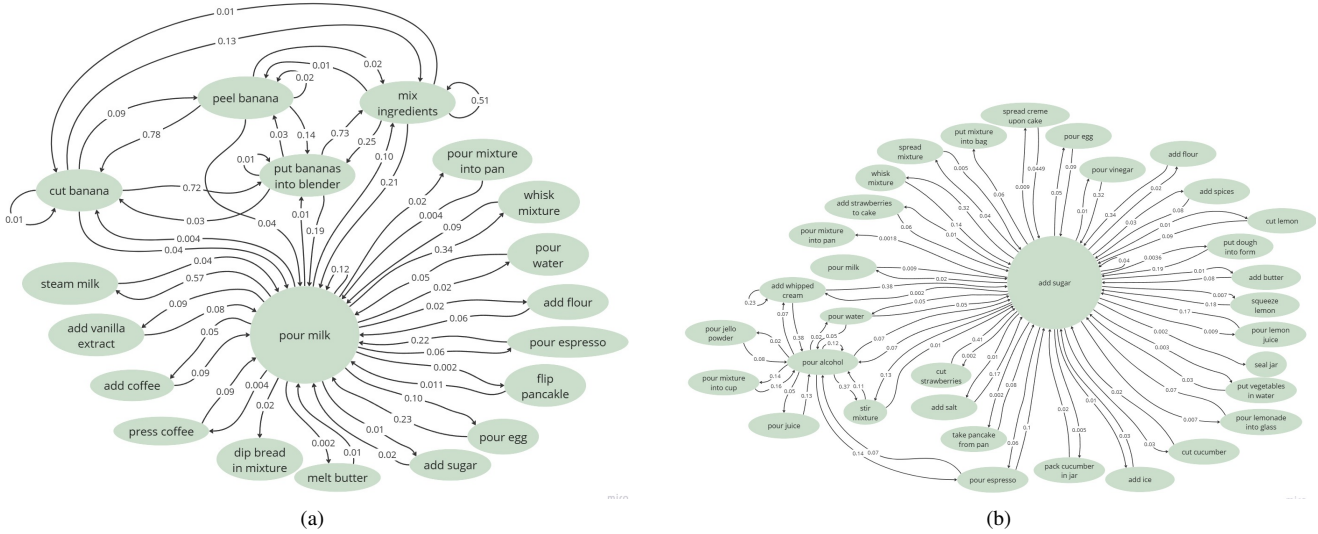


Figure S.1. **Probabilistic Procedure Knowledge Graphs (P²KG)** around the nodes ‘peel banana’ and ‘add whipped cream’ respectively up to a two-node depth. P²KG effectively captures the task-sharing steps, variability in transition probabilities between steps, implicit temporal and causal relationships of steps, as well as the existence of numerous viable plans given an initial step and an end step

Models	NIV ($T=5$)			NIV ($T=6$)		
	SR^\uparrow	$mAcc^\uparrow$	$mIoU^\uparrow$	SR^\uparrow	$mAcc^\uparrow$	$mIoU^\uparrow$
PDPP [50]	18.95	37.26	87.50	14.94	41.02	93.70
Ours ($R=2$)	21.58	39.79	91.66	17.53	43.62	93.75

Table S.2. **Performance of baselines and ours on the NIV dataset.** Our method demonstrates superior performance on all metrics

Model	SR^\uparrow	$mAcc^\uparrow$	$mIoU^\uparrow$
PDPP [50]	18.69	52.44	62.38
Ours ($R=1$)	20.38	55.54	64.03
Ours ($R=2$)	21.02	56.08	64.25
Ours ($R=3$)	20.22	56.19	63.15
Ours ($R=4$)	20.76	55.63	64.22
Ours ($R=5$)	20.37	55.43	63.93

Table S.3. **Parameter sensitivity study on the CrossTask dataset.** Performance of our method initially increases and then decreases as R continues to increase. An excessively large value for R may lead to the inclusion of less prominent paths in the conditions given to the planning model

for future work.

B. More Thorough Analysis

B.1 More Qualitative Results

Figure S.2 presents more qualitative results of our method compared with PDPP [50] across a range of procedural tasks, with a planning horizon set at $T=4$. In scenarios depicted in Figure S.2 (a), (c), and (d), the PDPP model

erroneously predicts the initial or final steps based on the given visual states, resulting in procedural planning failures. Our approach, however, incorporates a specialized step model designed to accurately predict these crucial first

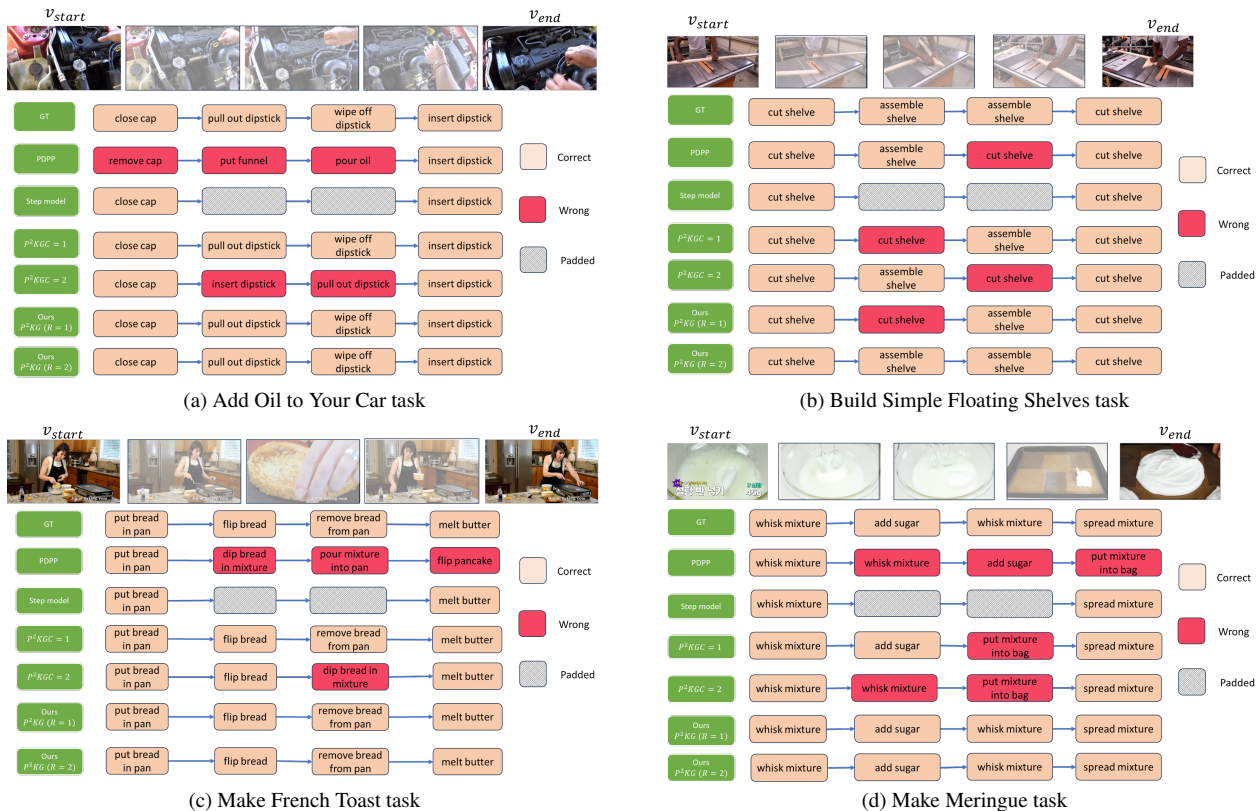


Figure S.2. **Qualitative Analysis of Different Procedural Tasks.** In the illustration, ‘ $P^2KGC = 1$ ’ and ‘ $P^2KGC = 2$ ’ indicates the first and second paths obtained from the probabilistic procedure knowledge graph respectively

and last steps. Furthermore, Figure S.2 highlights how our method benefits from the plan recommendations provided by the probabilistic procedure knowledge graph. These recommendations offer invaluable insights into feasible plans identified during training, thereby significantly enhancing our method’s capability in procedure planning at test time.

B.2 More Visualizations of the Probabilistic Procedure Knowledge Graph

Figure S.1 (a) and (b) show the sub-graphs in our probabilistic procedure knowledge graph (P^2KG) around the nodes ‘peel banana’ and ‘add whipped cream’ up to a two-node depth respectively. P^2KG effectively captures the task-sharing steps, variability in transition probabilities between steps, implicit temporal and causal relationships of steps, as well as the existence of numerous viable plans given an initial step and an end step.

B.3 Training Efficiency

Figure S.3 compares the training convergence of our planning model with PDPP [50]. We have plotted the loss values across the training epochs and indicated the epoch of convergence determined by the early stopping scheme.

Our model, with $R=2$ and $R=1$, converged at the 30th and 40th epochs, respectively, while the previous state-of-the-art method, PDPP, converged at the 60th epoch. Our model exhibited significantly faster training convergence compared to PDPP. The training efficiency of our method is achieved by leveraging the probabilistic procedure knowledge graph, which provides valuable context to facilitate the model’s learning process.

B.4 Analysis by the Step Transition Heatmap

Figure S.4 visualises the step transition matrices of the ground-truth training procedure plans, ground-truth testing procedure plans, and procedure plan predictions made by our method with $R=1$ on the test set, for the ‘Change a Tire’ task on the CrossTask dataset. The i-row-j-column depicts the probability of the transition from i-th action step to j-th action step. Darker color of the step transition heatmap indicates higher probability. The steps depicted in the heatmaps in order are: “brake on”:1, “get things out”:2, “start loose”:3, “jack up”:4, “unscrew wheel”:5, “withdraw wheel”:6, “put wheel”:7, “screw wheel”:8, “jack down”:9, “tight wheel”:10, “put things back”:11, “remove funnel”:12, “lower jack”:13, “put funnel”: 14, “wipe off

Convergence comparison between KEPP and PDPP

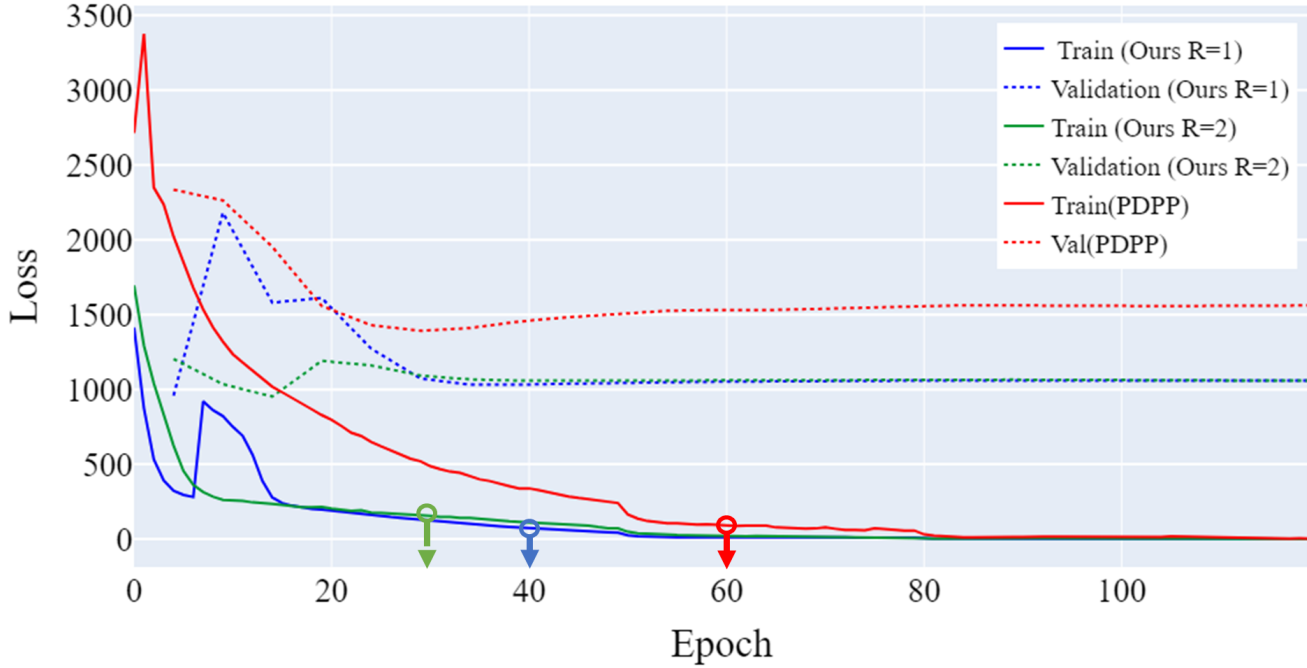


Figure S.3. **Training efficiency comparison between PDPP [50] and our model (KEPP).** These training and validation profiles demonstrate that our model exhibited significantly faster training convergence compared to PDPP. Our method with $R=2$ has faster convergence compared to $R=1$. The arrows indicate the epochs of convergence determined by the early stopping scheme

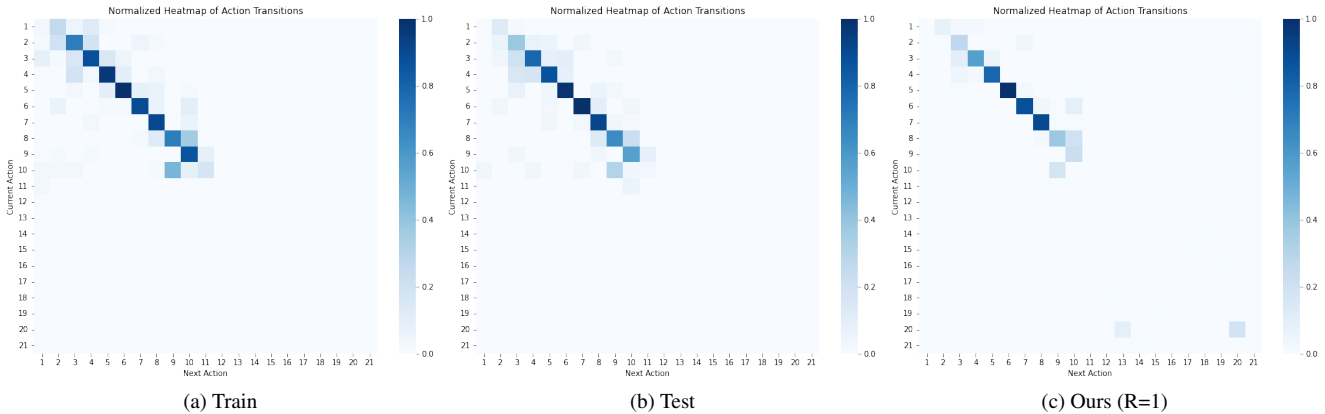


Figure S.4. **Step Transition Heatmaps on the CrossTask dataset of (a) the training set, (b) the testing set, and (c) procedure plan predictions made by our method on the test set.** The i -row- j -column depicts the probability of the transition from i -th action to j -th action. Darker color indicates higher probability. Please refer to Section B.4 for details regarding task and action names

dipstick”: 15, “close cap”:16, “insert dipstick”:17, “pour oil”:18, “pull out dipstick”:19, “raise jack”:20, “remove cap”:21.

Out of the 21 actions illustrated, first 11 actions belong to the ‘Change a Tire’ task while other actions are from several other tasks but highly relevant to the ‘Change a Tire’

task (e.g., ‘raise jack’:20 and “lower jack”:13). When comparing Figure S.4 (a) and (b), the distributions of action step transitions differ between training and testing. When comparing Figure S.4 (b) and (c), our method, which utilizes graph-structured training knowledge, reasonably predicts the step transition matrix on the test set.

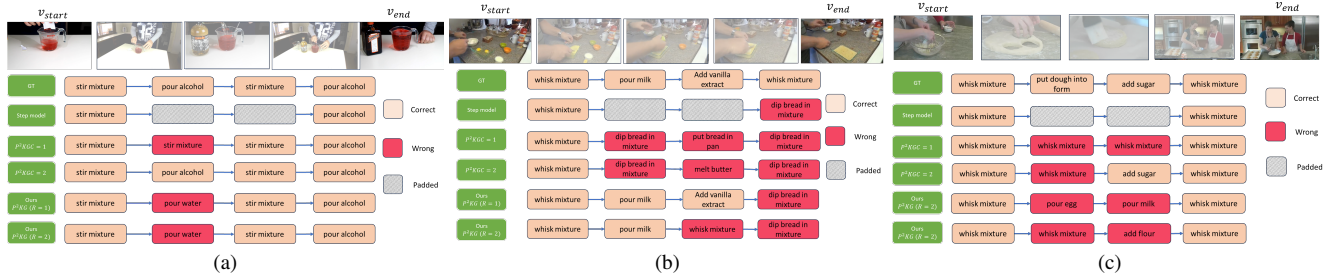


Figure S.5. **Failure Cases:** (a) when repetitive smaller action sequences exist within the procedure plan, (b) when a_1 and a_T have not been accurately predicted by the step model, and (c) when the start and end action steps are the same, and the probabilistic procedure knowledge graph fails to provide valuable plan recommendations because it overly encodes the repetitive actions

B.5 Limitations and Failure Cases

Figure S.5 illustrates three distinct failure case patterns in our model: (a) failure in prediction when repetitive smaller action sequences exist within the procedure plan, (b) failure in accurately predicting a_1 and a_T from the step model, and (c) failure in generating valuable probabilistic procedure knowledge graph paths because the graph overly encodes the repetitive actions when the start and end action steps are the same. Consistent with prior studies, cases involving repetitive actions or action sequences continue to pose challenges. Future studies could consider addressing these challenging scenarios.

The failure case analysis highlights the limitations of our approach. Our method depends on the precise prediction of both the initial and final steps by the step model, and it performs more effectively when the probabilistic procedure knowledge graph can offer valuable contextual information.

C. Method and Implementation Details

We will publicly release our code and trained models.

C.1 Diffusion Model Details

Standard Diffusion Model. A standard denoising diffusion probabilistic model [22] tackles data generation by establishing the data distribution $p(x_0)$ through a denoising Markov chain over variables $\{x_N \dots x_0\}$, starting with x_N as a Gaussian random distribution.

In the forward diffusion phase, Gaussian noise $\epsilon \sim \mathcal{N}(0, \mathbf{I})$ is progressively added to the initial, unaltered data x_0 , transforming it into a Gaussian random distribution. Each noise addition step is mathematically defined as:

$$x_n = \sqrt{\bar{\alpha}_n}x_0 + \epsilon\sqrt{1 - \bar{\alpha}_n} \quad (6)$$

$$q(x_n|x_{n-1}) = \mathcal{N}\left(x_n; \sqrt{1 - \beta_n}x_{n-1}, \beta_n\mathbf{I}\right) \quad (7)$$

where $\bar{\alpha}_n = \prod_{s=1}^n (1 - \beta_s)$ represents the noise magnitude, and $\{\beta_n \in (0, 1)\}_{n=1}^N$ denotes the pre-defined ratio of Gaussian noise added in each step.

Conversely, the reverse denoising process transforms Gaussian noise back into a sample. Each denoising step is mathematically defined as:

$$p_\theta(x_{n-1}|x_n) = \mathcal{N}(x_{n-1}; \mu_\theta(x_n, n), \Sigma_\theta(x_n, n)) \quad (8)$$

where μ_θ is parameterized as a learnable noise prediction model $\epsilon_\theta(x_n, n)$, optimized using a mean squared error (MSE) loss $L = \|\epsilon - \epsilon_\theta(x_n, n)\|^2$, and Σ_θ is calculated using $\{\beta_n\}_{n=1}^N$. During training, the model selects a diffusion step $n \in [1, N]$, calculates x_n via Eq. 6, then the learnable model estimates the noise and computes the loss based on the actual noise added at step n . After training, the diffusion model generates data akin to x_0 by iteratively applying the denoising process, starting from random Gaussian noise.

Conditioned Projected Diffusion Model. As we incorporate conditional information into the data distribution, these conditional guides can be altered during the denoising process. However, modifying these conditions can lead to incorrect guidance for the learning process, rendering conditional guides ineffective. To tackle this issue, the Conditioned Projected Diffusion Model has been introduced to ensure that guided information remains unaffected during denoising. In this approach, Wang et al. [50] introduce a condition projection operation within the learning process. Specifically, they enforce that visual observation conditions and additional condition dimensions remain unchanged during both training and inference by assigning them to their initial values. We have adapted their Conditioned Projected Diffusion Model as the architecture for both our step model and planning model in KEPP.

C.2 Implementation of KEPP

The step model for a_1 and a_T predictions and the planning model for procedure plan full-sequence prediction are trained separately. As mentioned in the main paper, for the step model, intermediate actions are padded in order to accurately predict a_1 and a_T . We use a U-Net based Conditioned Projected Diffusion Model [50] $f_\theta(x_n, n)$ as the

learnable model architecture for both of the step model and the planning model, and the training loss is:

$$L = \sum_{n=1}^N (f_{\theta}(x_n, n) - x_0)^2 \quad (9)$$

where x_0 denotes the initial, unaltered input and N denotes the total number of diffusion steps.

In line with the approach taken in [50], given that a_1 and a_T are the most relevant actions for the provided input visual states, we have modified the training loss by implementing a weighted MSE loss. This involves multiplying the loss by a weight matrix to give more emphasis to the predictions of a_1 and a_T . For the step model, we have chosen a weight of 10 for both a_1 and a_T . In the case of the planning model, we have assigned a weight of 5 to a_1 and a_T because the condition dimensions of intermediate steps in the probabilistic procedure knowledge graph path has a more significant impact on generating the full action step sequence. The default value in this weight matrix is 1.

The batch size is 256 for all the experiments. Our training regimen incorporates a linear warm-up strategy that is tailored to suit the varying scales of different datasets. For the results of models utilizing the precomputed features provided in CrossTask, we use 200 for the diffusion step and train the progress through a total of 12,000 training steps. The learning rate is gradually escalated to reach 8×10^{-4} over the initial 4,000 steps. Subsequent to this phase, we implement a learning rate reduction to 4×10^{-4} when reaching the 10,000th step.

When working with the S3D network-extracted features on the CrossTask dataset, the model similarly starts with a diffusion step of 200 but extends the training duration to 24,000 steps. The learning rate here ascends linearly to 5×10^{-4} within the first 4,000 steps, followed by a decay factor of 0.5 applied sequentially at the 10,000th, 16,000th, and 22,000th steps.

The NIV dataset, given its smaller size, necessitates a shorter training cycle of 6,500 steps, starting from a diffusion step of 50. We increase the learning rate linearly to 3×10^{-4} up until step 4,500, then introduce a decay by 0.5 at step 6,000.

For the COIN dataset, which is significantly larger in scale, the model undergoes an extended training sequence of 160,000 steps with the diffusion set at 200. Here, the learning rate experiences a linear surge to 1×10^{-5} within the first 4,000 steps. We implement a decay rate of 0.5 at the 14,000- and 24,000-step marks. After this point, the learning rate is maintained at a constant 2.5×10^{-6} for the remainder of the training process.

When obtaining mIoU, for CrossTask dataset we compute IoU on every single action sequence and calculates the average of these IoUs to obtain mean IoU similar to method

used in [50]. For COIN and NIV datasets, we compute mIoU on every mini-batch (batch size = 256) and calculate the average as the result similar to the approach used in [55].

In the scenario where paths from the probabilistic procedure knowledge graph are available between \hat{a}_1 and \hat{a}_T but it does not match the desired number of paths (R), then repetition of already available paths are considered to meet the desired path requirement. In scenarios where the combination of \hat{a}_1 and \hat{a}_T does not result in the inclusion of a path from the probabilistic procedure knowledge graph, the graph paths (P) are formulated as follows:

$$\text{Path Variations } (L) = [[[\hat{a}_1]^{T-M} \cdot [\hat{a}_T]^M], [[\hat{a}_1]^M \cdot [\hat{a}_T]^{T-M}]]$$

$$\text{Generated Paths } (P) = [L[i \bmod \text{len}(L)]] \text{ for } i \text{ in range } (R)$$

where T is the planning horizon, $M = T//2$, and path variations (L) are the two types of possible combinations of \hat{a}_1 and \hat{a}_T . For example if horizon (T) equals 5, then the path variations (L) possible are $[[\hat{a}_1, \hat{a}_1, \hat{a}_1, \hat{a}_T, \hat{a}_T], [\hat{a}_1, \hat{a}_1, \hat{a}_T, \hat{a}_T, \hat{a}_T]]$. So if one path ($R = 1$) is required as the condition for the planning model, generated path is $[\hat{a}_1, \hat{a}_1, \hat{a}_1, \hat{a}_T, \hat{a}_T]$, and if 2 paths are required ($R = 2$) as the condition for the planning model, generated paths are $[\hat{a}_1, \hat{a}_1, \hat{a}_1, \hat{a}_T, \hat{a}_T]$, and $[\hat{a}_1, \hat{a}_1, \hat{a}_T, \hat{a}_T, \hat{a}_T]$, and if 3 paths are required ($R = 3$) as the condition for the planning model, generated paths are $[\hat{a}_1, \hat{a}_1, \hat{a}_1, \hat{a}_T, \hat{a}_T]$, $[\hat{a}_1, \hat{a}_1, \hat{a}_T, \hat{a}_T, \hat{a}_T]$, and $[\hat{a}_1, \hat{a}_1, \hat{a}_1, \hat{a}_T, \hat{a}_T]$ likewise. The generated paths (P) are then aggregated through linear weighting into a single path to be given to the planning model as mentioned in Section 5 A.2.

C.3 Implementation of Ablations

Ablation on the probabilistic procedure knowledge graph. When the probabilistic procedure knowledge graph is not included as a condition, the model simplifies only to the planning model, ignoring the step model for generating \hat{a}_1 and \hat{a}_T . In this scenario, the planning model generates the action sequences using a diffusion process conditioned solely on the start and end visual observations.

Plan recommendations provided by the probabilistic procedure knowledge graph and LLM. To enhance the action prediction, we could incorporate LLM generated action sequence as a condition to our planning diffusion model as shown in Table 6 in the main paper. To generate the LLM action sequence we use the ‘llama-2-13b-chat’ model and query the model with the prompt:

```
“In the multi-step task that I am going to perform, I know {total_steps} steps are required, the first step is {start_action}, and the last step is {endaction} and I need to go from
```

{start_action} to {end_action}. Can you tell me the {total_steps} steps in the form "Step 1, ..., Step {total_steps}" so that I can follow in order to complete this {total_steps}-step task? Note that repetitive steps are possible".

In the above text prompt, ‘total_steps’ indicates the planning horizon, while ‘start_action’ denotes the step model-predicted start action \hat{a}_1 and ‘end_action’ denotes the step model-predicted end action \hat{a}_T . For a single $[\hat{a}_1, \hat{a}_T]$ pair occurring in the training or testing phase, we query the LLM three times and obtain the optimal action for each step in the sequence by finding the action with the highest occurrence. Then, the optimal sequence is queried back into the LLM for post-processing to check the realistic nature of the generated action sequence. The text prompt used for post-processing verification is as follows:

“Is the following action sequence possible? Note that repetitive steps are possible. Please answer only "Yes" or "No": {steps}”.

Here, ‘{steps}’ denotes the the generated steps from the first prompt. We then map the action steps generated from the LLM to the step vocabulary space of the given dataset. Specifically, the generated action steps from the LLM, as well as all of the possible action steps from the dataset, are embedded into a vector space utilizing the ‘bert-base-uncased’ model. For each action in the LLM-generated sequence, its semantically closest action step from the dataset is found in the vector space using the K-nearest neighbor (K=1) approach. The resulting generated action sequence is given as an additional input condition to the planning model similar to the P²KG condition.

In the situation where both the P²KG and LLM conditions are used for the planning model, the conditional visual states, LLM recommendation and the procedure plan recommendation from the P²KG are concatenated with the actions along the action feature dimension, forming a multi-dimensional array:

$$\begin{bmatrix} v_s & 0 & \dots & 0 & v_g \\ \tilde{a}_1 & \tilde{a}_2 & \dots & \tilde{a}_{T-1} & \tilde{a}_T \\ a_1^* & a_2^* & \dots & a_{T-1}^* & a_T^* \\ a_1 & a_2 & \dots & a_{T-1} & a_T \end{bmatrix} \quad (10)$$

where \tilde{a}_i denotes the action from the P²KG at i^{th} step and a_i^* denotes the action generated from LLM at i^{th} step.

Probabilistic procedure knowledge graph (P²KG) and Frequency-based procedure knowledge graph (PKG). The frequency-based procedure knowledge graph

(PKG) performs min-max normalization for the entire graph, and the optimal path between two nodes is the maximum weighted path. The path weight is calculated by summing all the individual edge weights between the two nodes. The probabilistic procedure knowledge graph (P²KG) has undergone output edge normalization, where the summation of probabilities of all the output paths from a node is 1. For example, if a node has four output edges (self-loop edges are also considered as output edges), and the weights along the edges are w_1, w_2, w_3, w_4 , then the probability of each edge is: $\frac{w_1}{w_1+w_2+w_3+w_4}, \frac{w_2}{w_1+w_2+w_3+w_4}, \frac{w_3}{w_1+w_2+w_3+w_4}, \frac{w_4}{w_1+w_2+w_3+w_4}$ respectively. The process of obtaining the highest probable path between two nodes is explained in Section 3.2.3 of the main paper.

C.4 Baselines

In the current study, we benchmark our proposed approach against several established state-of-the-art methods to conduct a comprehensive evaluation. Below, we describe the methods that serve as our baseline comparisons.

Random Strategy: This naive approach involves the stochastic selection of actions from the set of possibilities within the dataset to generate procedure plans.

Retrieval-based Technique: Upon receiving the visual observational inputs, this method employs a nearest-neighbour algorithm, leveraging the least visual feature space distance within the training corpus to extract a corresponding sequence of actions as the procedural blueprint.

WLTD0 [16] [‘CVPR 2018’]: Implemented via a recurrent neural network (RNN), this method sequentially forecasts the necessary actions based on the supplied pair of observations.

UAAA [1] [‘ICCV workshop 2019’]: Standing for a two-phased strategy, UAAA integrates an RNN with a Hidden Markov Model (HMM) to autoregressively estimate the sequence of actions.

UPN [45] [‘ICML 2018’]: This path-planning algorithm is tailored for the physical realm and acquires a plannable representational form for making informed predictions.

DDN [9] [‘ECCV 2020’]: The DDN framework operates as a dual-branch autoregressive model, honing in on an abstracted representation of action sequences to anticipate the transitions between states and actions in the feature space.

PlaTe [46] [‘RA-L 2022’]: An advancement of DDN, the PlaTe model incorporates transformer modules within its dual-branch architecture to facilitate prediction.

Ext-GAIL [7] [‘ICCV 2021’]: Ext-GAIL addresses procedural planning through reinforcement learning and decomposes the problem into a dual-stage challenge. The initial stage in Ext-GAIL is designed to yield time-invariant contextual information for the subsequent planning phase.

P³IV [55] [‘CVPR 2022’]: A transformative single-branch model, P³IV enriches its structure with a mutable memory repository and an additional generative adversarial network. It is capable of concurrently predicting the entire action sequence during the inference stage.

PDPP [50] [‘CVPR 2023’]: PDPP conceptualizes the task of procedure planning in instructional videos as analogous to fitting a probabilistic distribution. Echoing the P³IV, PDPP employs a holistic approach during the inference stage by forecasting the entire sequence of action steps concurrently.

SkipPlan [29] [‘ICCV 2023’]: Consider procedure planning as a mathematical chain problem. This model decomposes relatively long chains into multiple short sub-chains by bypassing unreliable intermediate actions. This transfers long and complex sequence functions into short but reliable ones.

E3P [49] [‘ICCV 2023’]: This uses procedural task (referred as ‘event’ in [49]) information for procedure planning by encoding task information into the sequential modeling process. E3P infers the task information from the observed states and then plans out actions based on both the states and the predicted task/event.